Mechanical and Viscoelastic Behavior of Natural Rubber and Carboxylated Styrene-Butadiene Rubber Latex Blends

Ranimol Stephen,[1] K. V. S. N. Raju,[2] Sobha V. Nair,[3] Siby Varghese,[4] Zachariah Oommen,[5] Sabu Thomas[3]

[1]Department of Chemistry, C. M. S. College, Kottayam 686 001, Kerala, India
[2]Organic Coatings and Polymers Division, IICT, Hyderabad 7, Andhra Pradesh, India
[3]School of Chemical Sciences, Mahatma Gandhi University, Priyadarshini Hills P.O., Kottayam 686 560, Kerala, India
[4]RCPT Division, Rubber Research Institute of India, Kottayam 686 009, Kerala, India
[5]Department of Criminal Justice, Albany State University, Albany, Georgia 31705-2796

ABSTRACT: The morphology, mechanical and viscoelastic behavior of latex blends of unvulcanized natural rubber (NR) with carboxylated styrene-butadiene rubber (XSBR) were investigated, with special reference to the effect of the blend ratio, temperature, and frequency. Mechanical properties like tensile strength, modulus, and elongation at break were also studied. As the XSBR content increased, the tensile strength increased up to a 50:50 NR/XSBR ratio and then decreased as a result of the self-curing nature of XSBR. The dynamic mechanical properties of these latex blends were analyzed for loss tangent, storage modulus, and loss modulus. The entire blend yielded two glass-transition temperatures, which corresponded to the transitions of individual components, indicating that the system was immiscible. To determine the change in modulus with time, a master curve of 50:50 NR/XSBR blends was plotted. Time–temperature superposition and Cole–Cole analysis were done to understand the phase behavior of the latex blends. The experimental and theoretical values of storage modulus of blends were compared using the Kerner and Halpin–Tsai models. With the help of optical micrographs, attempts were made to correlate the morphology and viscoelastic behavior of these blends. © 2003 Wiley Periodicals, Inc. J Appl Polym Sci 88: 2639–2648, 2003

Key words: latices; blends; glass transition; mechanical properties; visoelastic

INTRODUCTION

Latex stage blending of two polymers has some advantages because it is the easiest way to blend, resulting in a finer scale of dispersion. Hence, blending of latices has become a common practice to improve the processing as well as the ultimate properties. Latex blends can be characterized by rheological, mechanical, and viscoelastic property measurements. Shundo et al.[1] correlated the properties of unvulcanized and vulcanized blends of NR and SBR prepared by solution blending, latex blending, roll blending, and banbury mixer blending. The properties of NR and SBR latices had been reported earlier by Blackley and Charnock.[2–4] The mechanical properties of polymeric materials are considered the most important of all the physical and chemical properties because it has desirable mechanical properties at an economical cost.[5]

The morphology of polymer blends depends on the volume fraction and viscosity of the individual components.[6] The impact of the morphology of polymer blends on its end-use applications has been reported.[7–8] Thomas and coworkers[9–11] investigated the morphology of many polymer blends. They found that the mechanical and dynamic properties of polymer blends only could be explained by their morphology.

Dynamic mechanical tests are useful for studying the miscibility between two polymers.[11] The viscoelastic behavior of polymers is characterized by dynamic mechanical analysis. Dynamic mechanical parameters such as storage modulus, loss modulus, and the loss tangent of the polymers have been used to determine the glass-transition region, relaxation modulus, degree of crystallinity, molecular orientation, crosslinking, phase separation, and so forth. Knowledge of the viscoelastic properties of polymeric materials is important because most critical engineering applications are a combination of storage and loss modulus that dictate the failure of a polymer and its toughness under a given deformation history.[12] Ashby[13] did a good review of the engineering properties of a wide range of materials, allowing the mechanical properties of polymers to be compared with other solids. There have been many articles on the importance of both

theoretical and experimental approaches to the dynamic mechanical properties in polymer processing.[14–15] The crucial role of these properties in polymer blends is enabling an understanding of miscibility and phase behaviors. The miscibility of the blends can easily be investigated from the shift in T_g.[16] If the system is miscible, only one T_g is obtained at a glass-transition intermediate between the two components, whereas broadening of the transition peak will occur or the presence of two peaks indicates partial miscibility and immiscibility of the two components.[17] It has been reported that dynamic mechanical techniques can provide a meaningful correlation between molecular structure and mechanical property.[18]

Very recently, Varkey et al.[19] investigated the viscoelastic properties of NR/SBR blends at different frequencies and temperatures. The phase behavior of the blends was evaluated using a master curve and Cole–Cole plots. All the NR/SBR blends have shown two distinct glass-transition temperatures, indicating that the system is immiscible. Thomas and coworkers[9–10] also studied the viscoelastic behavior of nitrile rubber (NBR)/ethylene–vinyl acetate (EVA) copolymer and natural rubber (NR)/EVA copolymer blends. They explored the miscibility and viscoelastic properties of these blends, especially the effect of the blend ratio.

The important role of dynamic mechanical analysis in understanding the behavior of rubber blends is widely accepted. According to the literature DMA is a reliable tool for getting unambiguous temperature of the dynamic glass transitions and rubber plateaus.[20] Many researchers[21–23] have taken both theoretical and experimental approaches to investigating these properties of the blends.

There have been a number of reports regarding the rheological, transport, thermal, morphological, and viscoelastic properties of NR, NR/SBR, ENR, and ENR/SBR latices and their blends.[19,24–29] Carboxylated SBR (XSBR) latex has shown enhanced colloid stability and increased tolerance with the addition of large quantities of mineral fillers, which simplifies its processibility.[30] To date, no systematic study on the viscoelastic properties of NR/XSBR blends has been reported. The purpose of the present study was to investigate the morphology, viscoelastic behavior, and mechanical properties of NR/XSBR unvulcanized latex blends with reference to their blend ratio. Because of the polarity of XSBR, it showed better adhesion to polar substrates such as textile fibers, paper fibers, and metals, enhanced polymer tensile strength, and improved resistance to hydrocarbon oils.[31] Blending of NR with XSBR can easily modify the properties of NR. The detailed investigation of the mechanical properties of NR/XSBR latex blends in the current study showed a positive deviation.

TABLE I
Details of Materials Used

Centrifuged natural rubber (NR) latex	
Supplier	Gaico Ltd., Kuravilangadu, Kerala, S India
Dry rubber content (DRC) (%)	60
Total solid content (TSC) (%)	61.25
Alkalinity (%)	0.75
Volatile fatty acid (VFA) number	0.05
Mechanical stability	Good
Manganese content	Traces
Magnesium (ppm)	29
Molecular weight	5×10^5

Carboxylated styrene butadiene rubber (XSBR) latex (PLX-802)	
Supplier	Apar Industries Ltd., Bombay, Maharashtra, India
Dry rubber content (DRC) (%)	47
Total solid content (TSC) (%)	50.66
Styrene content (%)	59
pH	8.60
Mechanical stability	Good
Molecular weight	$80–160 \times 10^3$

EXPERIMENTAL

Materials used

Centrifuged natural rubber (NR) latex with 60% dry rubber content (DRC) was supplied by Gaico Ltd., Kuravilangadu, Kerala, India. Carboxylated styrene butadiene rubber (XSBR) latex (PLX-802) was supplied by Apar Industries Ltd., Bombay, India. The basic characteristics of these two latices are given in Table I.

Preparation of blends

The blending of NR and XSBR latices was done at ambient temperature using a mechanical stirrer. It was then kept for 1 h in order to ensure homogenization and also the sedimentation of impurities. Films with a uniform thickness were obtained by casting on a glass plate, and they were allowed to dry at room temperature. NR and XSBR latices were blended in varying compositions according to their DRC. The blends were designated as N_{70}, N_{50}, and N_{30}, respectively, where N denotes the weight percent of NR. The details of the blending are shown in Table II.

Optical microscopic studies

The morphology of the NR/XSBR blends was studied using an optical microscope axioplan from Zeiss (Akron, OH).

TABLE II
Formulation of Unvulcanized NR/XSBR Latex Blending

	N_{100}	N_{70}	N_{50}	N_{30}	N_0
60% Centrifuged NR latex	100	70	50	30	-
47% XSBR latex	-	30	50	70	100
10% KOH solution	1	1	1	1	1

TABLE III
Domain Average Diameter of N_{30} and N_{70} Blends

Sample	$\bar{D}n$ (μm)	$\bar{D}s$ (μm)	$\bar{D}v$ (μm)	$\bar{D}w$ (μm)	PDI
N_{70}	0.27	0.28	0.29	0.29	1.1
N_{30}	0.57	0.61	0.64	0.66	1.2

Mechanical property measurements

Tensile testing was done in an Instron Universal Testing Machine (model 1121) using dumbbell-shaped samples from cast films of unvulcanized NR/XSBR latices and their blends. The method followed for testing was ASTM D 412-87. The test was conducted at a crosshead speed of 500 mm/min with a 3-cm intergrip distance. In each case five samples were tested and the average value reported. The tension set after failure was calculated according to the ASTM.

Dynamic mechanical thermal analysis (DMTA)

Viscoelastic properties were measured using a Rheometric Scientific DMTA 1V analyzer (IICT, Hyderabad, Andhra Pradesh, India). The testing temperatures were in the range of −100°C to 100°C. The measurements were carried out in a tension mode at 1, 5, and 10 Hz for all homopolymers at a heating rate of 1°C/min.

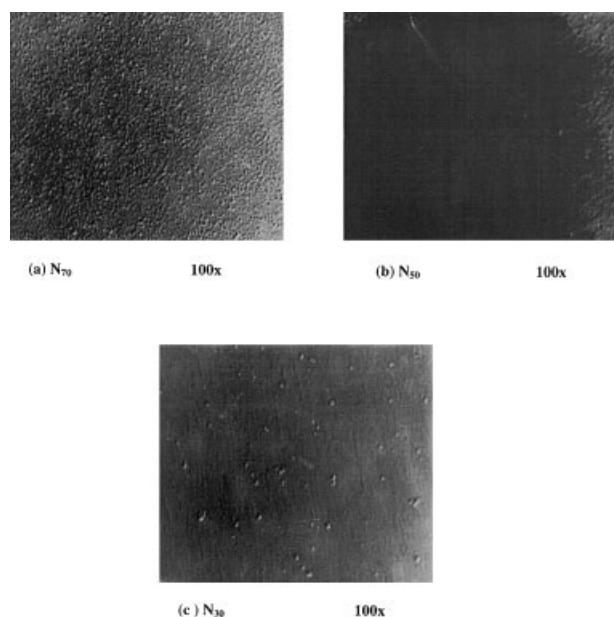**Figure 1** Optical micrographs of NR/XSBR latex blends: (a) N_{70} latex blend; (b) N_{50} latex blend; and (c) N_{30} latex blend.

RESULTS AND DISCUSSION

Morphology of blends

The major factors affecting the morphology of blends are composition, interfacial tension between the phases, and viscosity of the individual components. The coalescence of the particles in the dispersed phase depends mostly on the viscosity of the matrix.

The optical micrographs (magnification 100x) of unvulcanized NR/XSBR latex blends are given in Figure 1(a–c). In the N_{70} [Fig 1(a)] blends the XSBR phase was dispersed in the continuous NR matrix. Because the viscosity of the continuous NR phase was higher than that of the dispersed XSBR phase, the coalescence of the particles was not very predominant in the N_{70} blends. The NR phase was dispersed in the XSBR matrix in the N_{30} blends [Fig 1(c)]. The size of the dispersed NR particles in N_{30} was much higher than the dispersed size of the XSBR in the N_{70} blend. This is because of the great extent of coalescence as a result of the low viscosity of the XSBR. This can also be explained based on the capillary number,

$$Ca = \frac{\gamma \eta_m D}{2\Gamma} \tag{1}$$

where D is the diameter of the droplet, γ is the shear rate, η_m is the matrix viscosity, and Γ is the interfacial tension. The NR/XSBR latex blends with a 50:50 ratio exhibited cocontinuous morphology, meaning both phases are continuous [Fig. 1(b)]. A clear picture of this can be obtained from the $\bar{D}n$, $\bar{D}v$, $\bar{D}s$, and $\bar{D}w$ values of N_{70} and N_{30} latex blends, which are shown in Table III.

Mechanical properties

NR/XSBR unvulcanized latex blends have better mechanical properties than their individual components. Figure 2 shows the stress–strain behavior of unvulcanized NR/XSBR latex blends under tension. The stress–strain curves give an idea of the mode of deformation of the blends under an applied load. As the XSBR content in the blend increased, the stress value increased with strain and then decreased after attaining maximum. Compared with synthetic latices, except XSBR, NR usually showed a higher tensile
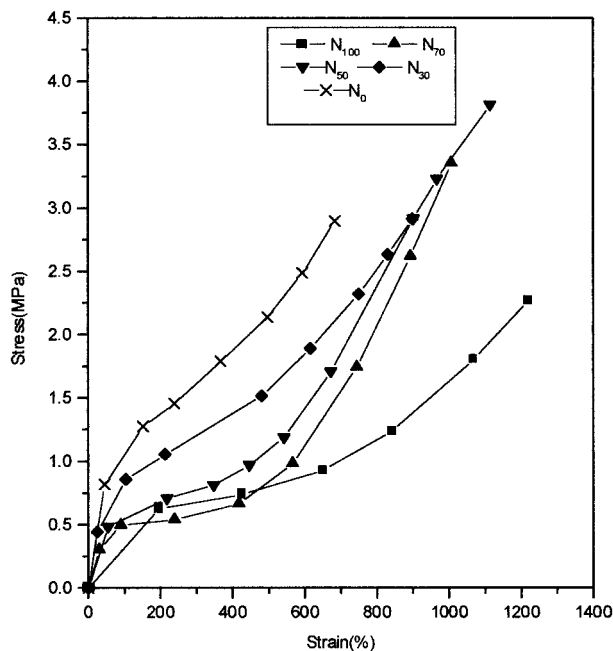
Figure 2 Stress–strain behavior of unvulcanized NR/XSBR latex blends.

strength because of its strain-induced crystallization. In this case, the high strength of XSBR can be attributed to the self-curing nature of XSBR blends. In addition, the strength of cohesion in XSBR is much higher than in NR because of its high polarity. The crossovers in the stress–strain curves can be explained by the stress transfer between the two phases, which depends on adhesion at the interface, which is clearly supported by the increased mechanical properties. This is also related to the morphology of the system.

The variation in tensile strength with composition of the NR/XSBR latex blends is shown in Figure 3—positive deviation from the additivity line can be seen. It has been shown by the tensile strength, tear strength, and puncture resistance that certain synthetic polymer latices added to NR latex are able to effect some degree of reinforcement.[32] King[33] reported that poly(vinyl chloride) particles added to NR latex as latices were able to enhance tensile strength and tear strength of postvulcanized films. Blackley[32] concluded that some structuring of the particles was likely to be conducive to reinforcement. Popoola[34] used experimental methods to investigate extensively the possibilities of reinforcement of NR latex films by another latex and also of films derived from two types of synthetic latices. Because of the self-curing nature of XSBR latex, it gives a higher tensile strength than does NR latex.

We found that the N_{50} blend showed maximum tensile strength and that further addition of XSBR reduced this tensile strength. This result is associated

with the cocontinuous nature of the two phases. In a cocontinuous interpenetrating system both phases take part in the load-bearing process. Therefore, there is no question of transferring the stress across the interface. Films obtained from XSBR latex are rigid in nature compared with those from NR. During film formation the rigid phase of the rubbery polymer tends to mix at the molecular and segmental levels with the macromolecules of the rubber matrix. Thus, it will enhance the tensile strength of blends up to N_{50}; after that, no reinforcement at all is possible, so tensile strength decreases with a further addition of XSBR. The modulus of the NR/XSBR blends in our study increased with an increase in XSBR content (Fig. 3). The elongation at break (Fig. 4) was higher for N_{100}, and, as expected, it decreased with an increase in XSBR content. This occurred because the adhesion at the interface decreased. The values of tension set after failure (Fig. 4) decreased as the XSBR content within the system increased. The recovery of the system was measured after 1 h.

Viscoelastic properties

Properties such as storage modulus (E'), loss modulus (E''), and damping (tan ∂) of unvulcanized NR/XSBR blends were evaluated over a wide range of temperatures and frequencies. Investigations of the temperature dependence of viscoelasticity have considerable practical importance and provide evidence for a molecular interpretation of viscoelastic behavior as the material changes from a glassy to a rubberlike state.
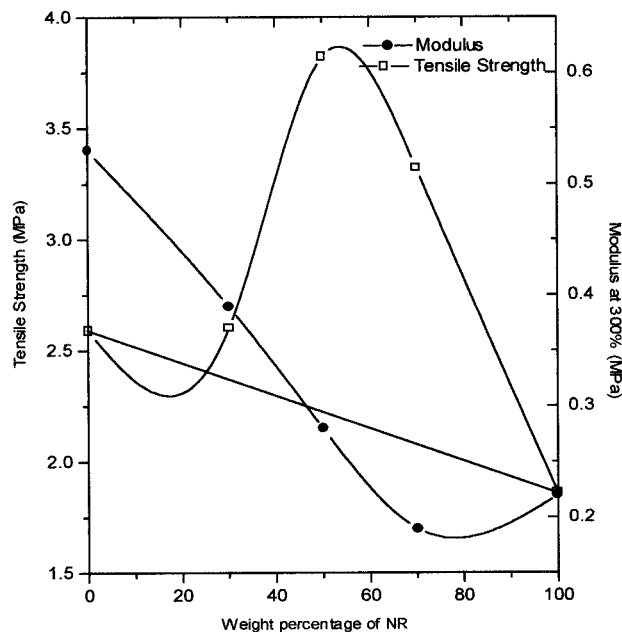

Figure 3 Variation of tensile strength and modulus of NR/XSBR latex blends with composition.
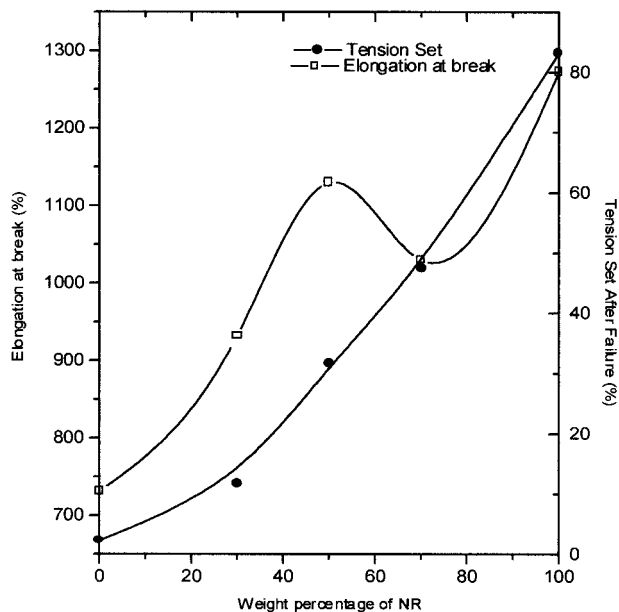
Figure 4 Effect of blend ratio on elongation at break and tension set values of NR/XSBR latex blends.

NR latex possesses higher damping values than XSBR latex. The damping behavior of blends is less than that of its individual components at both phases. Hence, it will be useful for the manufacture of low damping materials. The NR/XSBR blends were immiscible and showed two T_g values, which corresponded to the NR and XSBR phases.

The tan ∂ versus temperatures of the NR/XSBR blends is shown in Figure 5. These curves show two peaks to be those of a two-phase system; each peak is characteristic of the glass transition of one of the components,[35] indicating that the system is immiscible. The tan ∂ values can be selected from the peak position, and the T_g values are taken from the corresponding temperature of the peak for each phase. The T_g of the NR phases in the N_{70} blend was $-59°C$ at 1 Hz, whereas that of the XSBR phase was $15°C$. The transition temperatures of the pure components were $-52°C$ and $23°C$, for the NR and XSBR phases, respectively. The shift in T_g values of the blends with composition revealed the partial miscibility of the components.[36] Compared with SBR, XSBR showed a higher transition temperature because of its polarity and its self-crosslinking nature. All the observed transition temperatures for both phases at different blend ratios and at different frequencies are given in Table IV. In all cases the loss tangent values and transition temperatures increased with frequency.

The peak areas of the tan ∂ curves are given in Table V. There was a drastic change in the peak area of the NR phase on blending unlike with the XSBR phase. This is an indication of the extent of mobility of the macromolecular chain segments at the transition tem-

perature.[36] Any restriction in the main chain mobility in the polymer is expected to decrease the area under the curve. The drastic decrease in peak resulted from the self-curing behavior of XSBR latex, which formed networks within the system. Thus, the molecular mobility of the polymer chain segments were restricted at the transition temperature.

Figure 6 shows the tan ∂_{max} values of NR/XSBR blends with weight percent of NR. From the curve it can be seen that the tan ∂_{max} values of the NR phase decreased with an increase in the XSBR content of the blends—that is, NR had the highest damping values and the decrease was sharper when the XSBR content was 50% or greater. This can be attributed to the amorphous nature of NR compared with XSBR. The sharp decrease in damping value in the N_{50} blend was a result of the cocontinuous morphology of the composition [Fig. 1(b)]. This observation also supports the cocontinuous morphology of the system. Generally, the damping values decreased with an increase in crystallinity. For the N_{70} blend it showed a minimum, then it decreased for the N_{50} and N_{30} blends with an increase in XSBR content—that is, the tan ∂_{max} values of the XSBR phase increased with a decrease in NR content.

The values for storage modulus, E', for various blends over a wide range of temperatures are shown in Figure 7. The two steps of the modulus–temperature curve are characteristic of immiscible two-phase systems. The curves of all the compositions have three distinct regions: glassy (from $-75°C$ to $-65°C$), tran-
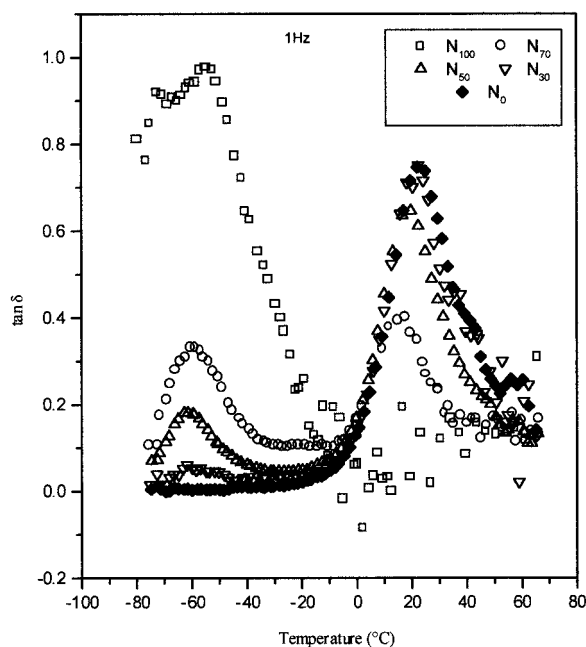

Figure 5 Tan δ versus temperature curve of unvulcanized NR/XSBR latex blends.

TABLE IV
Viscoelastic Properties of Unvulcanized NR/XSBR Latex Blends

Samples	Frequency (Hz)	tan δ_{max} NR phase	tan δ_{max} XSBR phase	T_g (°C) from tan δ_{max} NR phase (°C)	T_g (°C) from tan δ_{max} XSBR phase (°C)	T_g from E'' peak temperature (°C) NR transition (°C)	T_g from E'' peak temperature (°C) XSBR transition (°C)
N_{100}	1	0.99	—	−52.2	—	−63.6	—
	5	1.13	—	−51.9	—	−63.9	—
	10	1.16	—	−51.7	—	−61.3	—
N_0	1	—	0.76	—	23.8	—	5.6
	5	—	0.87	—	26.6	—	8.9
	10	—	1.03	—	31.2	—	10
N_{70}	1	0.34	0.42	−59.4	15.7	−58.9	6.1
	5	0.46	0.49	−58.3	19.5	−57.4	9.3
	10	0.47	0.53	−57.9	21.7	−57.0	7.4
N_{50}	1	0.21	0.67	−61.6	19.5	−62.1	5.6
	5	0.28	0.72	−61.3	24.2	−61.0	8.2
	10	0.33	0.79	−59.2	25.4	−61.66	8.7
N_{30}	1	0.08	0.77	−61.6	20.5	−61.0	5.0
	5	0.15	0.85	−61.7	24.2	−60.4	8.2
	10	0.16	0.91	−60.4	23.8	−60.4	7.4

sition (NR phase; from −65°C to −50°C), and rubbery. The transition region for the XSBR phase is between −15°C to −25°C at a frequency of 1 Hz. The modulus of the blends decreased with an increase in NR content. Compared with the other blends, the N_{50} blend showed the highest storage modulus because of the cocontinuous nature of the two phases. The value of E' was found to decrease with a rise in temperature as a result of the decrease in stiffness of the sample.

The values of the loss modulus, E'', of the NR/XSBR unvulcanized latex blends are shown in Figure 8. The main chain mobility in the polymer can be understood from looking at the curve of area under the loss modulus versus temperature.[37] As might be expected, the loss moduli increased sharply up to the transition zone until they attained maxima, then decreased with temperature. This curve shows the same trend as that of the tan ∂ versus temperature curve. The E'' peak temperature is more or less the same as that of the transition temperature obtained from the tan ∂ versus temperature curve. The sharp loss peaks indicate that the system components are immiscible. The E'' peak temperatures of various blends at different frequencies are shown in Table IV.

TABLE V
Peak Area of NR, XSBR, and Their Blends from tan δ Curves

Sample	Peak area NR phase	Peak area XSBR phase
N_{100}	32.44	—
N_{70}	4.059	4.143
N_{50}	2.48	2.48
N_{30}	0.07311	0.9414
N_0	—	4.818

Time–temperature superposition

The two experimental variables available in the measurement of viscoelastic properties are temperature and time.[12,17,38] Constructing a master curve makes it possible to easily understand the complete modulus–time behavior of a polymeric material. Master curve construction is based on the time–temperature correspondence principle. The data collected at one temperature can be superimposed on data taken at a different temperature by horizontal shifts.[39]
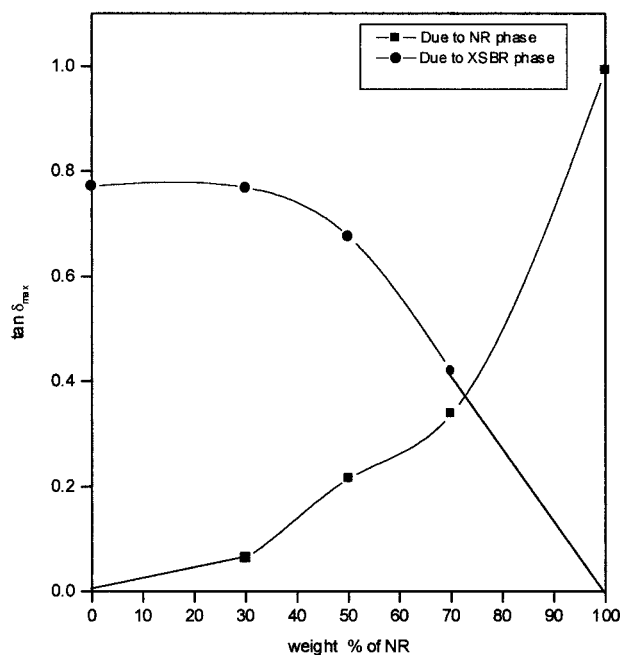

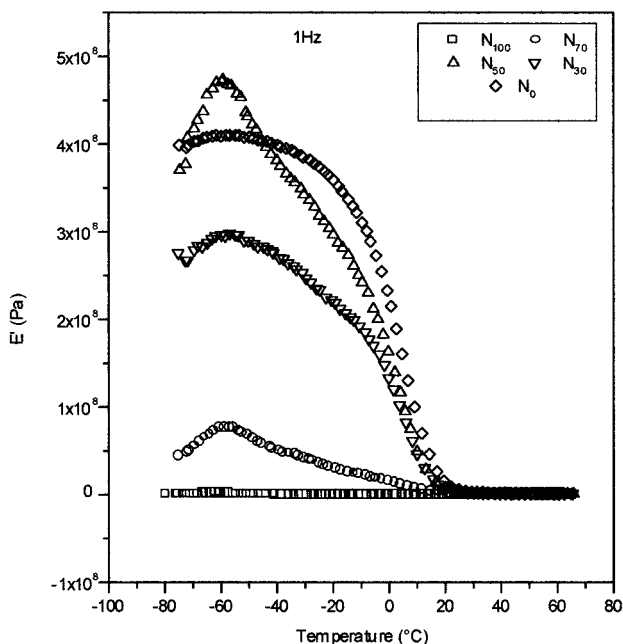**Figure 6** Effect of weight percent of NR on damping values of NR/XSBR latex blends.
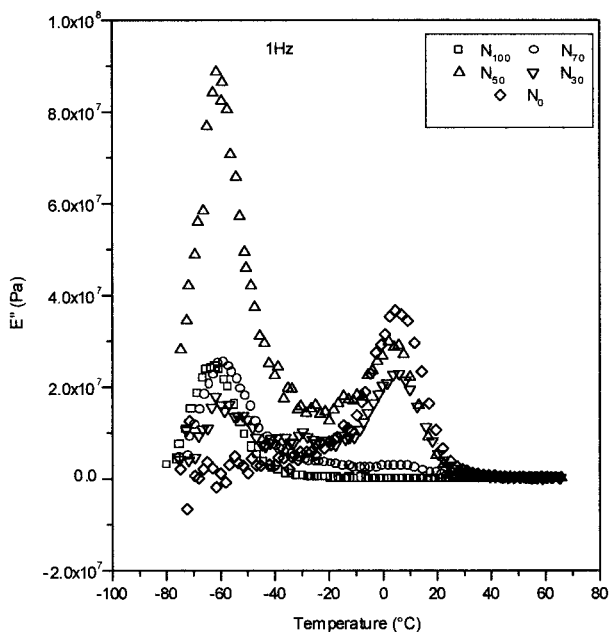
Figure 7 Variation of storage modulus (E') of NR/XSBR latex blends with temperature.

Figure 9 Log t versus log E' curves of N_{50} blends at different temperatures.

To construct a master curve it is necessary to pick one temperature, suppose T_1, as the reference temperature. The shift factor is a function of temperature and hence designated as a_T. All other experimental curves, each at a particular temperature are then shifted horizontally, that is, along the time axis until it overlaps the curve with the reference temperature, T_1. The shift factor characterizes the rate of the relaxation mecha-

nism at temperature T_1 in comparison with the rate at a higher temperature, T_{1+1}. From this the log a_T values for all temperature can be determined.

The viscoelastic properties at a given frequency, f, are quantitatively equivalent to those of an experiment carried out over time $t = 1/(2\pi f)$. Figure 9 shows the log t versus log E' curves of N_{50} blends at different temperatures. The temperature 0°C, was used the reference temperature for the N_{50} blends. The master curve was constructed by plotting $\log(t/a_T)$ versus $\log(ET_0/T)$ (Fig. 10), where E is the storage modulus at a particular temperature, T_0 is the reference temperature on the Kelvin scale, and T is the temperature of the experiment. The master curve explains the change in modulus with time.

Cole–cole analysis

Cole–Cole analysis of the blends can provide some knowledge about the miscibility of components. The Cole–Cole diagram of viscoelastic response for amorphous polymers is asymmetric, presenting the time dependency of viscoelastic behavior.[40] It was reported[41] that a homogeneous system shows a semicircle diagram, whereas a two-phase system shows two modified semicircles. Figure 11 shows the Cole–Cole plot for the N_{50} unvulcanized blends. In this case the system gave two modified semicircles. This can be attributed to the immiscibility of the two components.
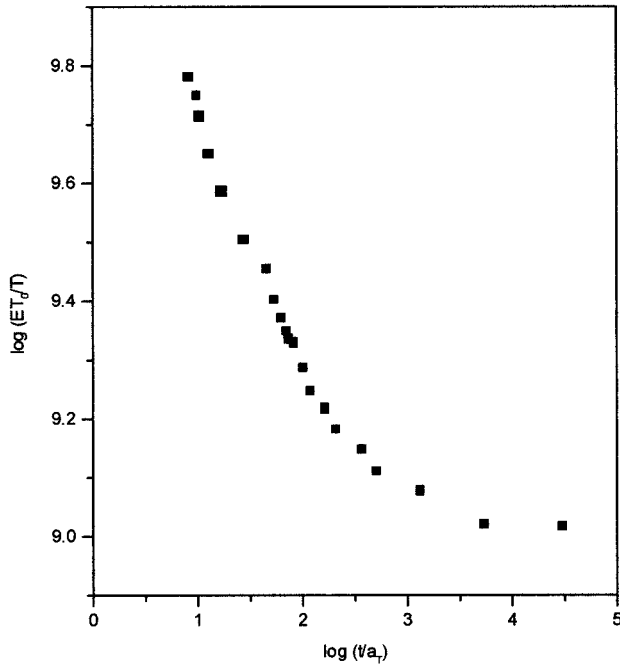

Figure 8 Loss modulus (E'') peak of NR/XSBR latex blends with temperature.

Figure 10 Master curve of N_{50} blends.

Theoretical modeling of dynamic properties

The theoretical modeling of polymer blends will help in the designing of materials for engineering applications. The objectives of comparing the theoretical and experimental values are to understand and to predict the mechanical properties and morphology of the system.[42–43]

The applicability of the Kerner and Halpin–Tsai models has been discussed for NR/XSBR latex blends. These models can be used to predict the viscoelastic behavior of rubber–rubber blends.[44–45]

The Kerner[46] equation is given by

$$E_b = E_m \left[\frac{\dfrac{\phi_d E_d}{[(7 - 5v_m)E_m + (8 - 10v_m)E_d]} + \dfrac{\phi_m}{15(1 - v_m)}}{\dfrac{\phi_d E_m}{[(7 - 5v_m)E_m + (8 - 10v_m)E_d]} + \dfrac{\phi_m}{15(1 - v_m)}} \right]$$

(2)

where E_b is the modulus of the blend, E_m is the modulus of the matrix, E_d is the modulus of the dispersed phase, ϕ_d is the volume fraction of the dispersed phase, ϕ_m is the volume fraction of the matrix, and v_m is the Poisson ratio for the rubber zone (the value of the Poisson ratio is usually considered as 0.5).

According to the Halpin–Tsai[47–49] model

$$\frac{M_1}{M} = \frac{(1 + A_i B_i \phi_2)}{(1 - B_i \phi_2)}$$

(3)

where

$$B_i = \frac{(M_1/M_2 - 1)}{(M_1/M_2 + A_i)}$$

(4)

A_i is 0.66, M is the modulus, and ϕ is the volume fraction; the subscripts 1 and 2 denote components 1 and 2, respectively.

Figure 12 shows the comparison of the theoretical and experimental values of the N_{30} and N_{70} latex blends. The theoretical values obtained were lower than those for the experimental values at low temperatures, whereas at higher temperatures there was good agreement between the experimental and theoretical values. Because of the higher storage modulus of XSBR latex, the N_{30} blend showed higher values compared with the N_{70} blends. As the XSBR content increased, the system showed more elastic behavior because of the self-curing nature of XSBR latex. The morphology of the blends [Fig. 1(a–c)] also provided support for the theoretical modeling because the system was considered as a phase dispersed in a continuous matrix. In both the N_{70} and N_{30} blends one phase was dispersed in another continuous matrix. At low temperatures the Halpin–Tsai model of N_{30} and N_{70} blends fit better with the experimental curve than did the Kerner model. But at higher temperatures both models matched the experimental results well.

CONCLUSIONS

Blends of NR and XSBR latices were prepared by mechanical blending. The mechanical properties, mor-
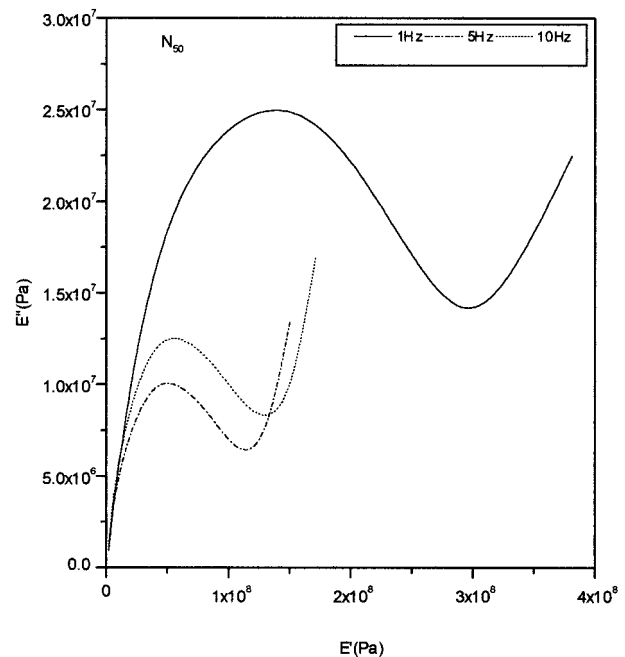

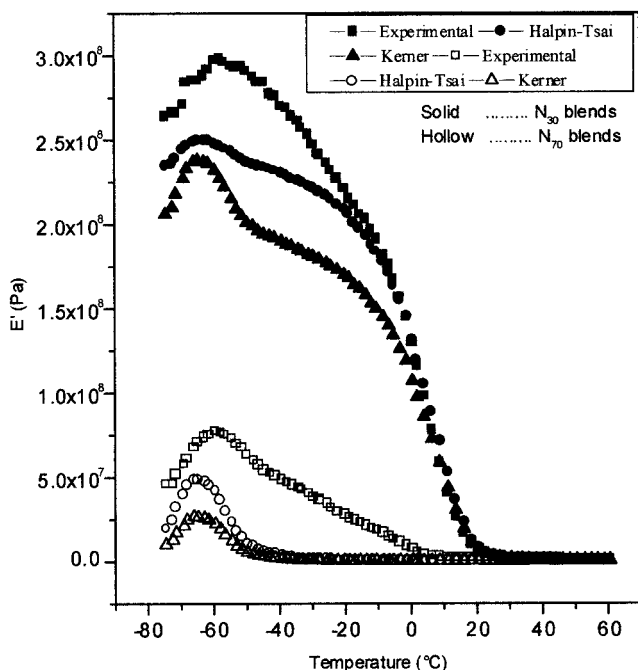**Figure 11** Cole–Cole plot of N_{50} blends.

Figure 12 Comparison of theoretical experimental storage modulus of N_{30} and N_{70} latex blends.

phology, and viscoelastic properties such as damping, storage modulus, loss modulus, and glass-transition temperatures of these blends were studied. Finally, the viscoelastic properties were theoretically correlated.

The tensile strength of the NR/XSBR latex blends increased with an increase in XSBR content up to N_{50}, then decreased because of the self-curing nature of XSBR content, whereas the modulus increased continuously with XSBR content. Elongation at break decreased with an increase in XSBR content.

The morphology of blends explains that in the N_{70} and N_{30} blends, the XSBR phase was dispersed in the NR matrix and the NR phase dispersed in the XSBR phase, respectively. An optical micrograph of the N_{50} blend showed a cocontinuous morphology.

The loss tangent curve of the blends showed two transition peaks corresponding to the individual components, indicating the system is immiscible. The damping value decreased with an increase in XSBR content, whereas it increased with an increase in frequency. An idea of the mobility of chain segments at the transition temperature could be obtained from the peak area of the tan ∂ curves.

The storage modulus of the system increased with an increase in XSBR content. The time–temperature superposition curve was constructed, and the shift factor was determined by using a reference temperature. The master curve of the N_{50} blend revealed a change in the modulus of the system with time. The

Cole–Cole plot showed two modified semicircles, indicating the system was heterogeneous.

The theoretical and experimental storage modulus values were compared using Kerner and Halpin–Tsai models. It is clear that in N_{70} and N_{30} blends the experimental values were higher than the theoretical values at low temperatures. This can be explained by the self-curing nature of XSBR latex. However, at ambient temperatures the theoretical and experimental values were in considerable agreement.

References

1. Shundo, M.; Imoto, M.; Minoura, Y. J Appl Polym Sci 1964, 10, 939.
2. Blackley, D. C.; Charnock, R. S. J Int Rubber Ind 1969, 7, 151.
3. Blackley, D. C.; Charnock, R. S. J Int Rubber Ind 1973, 7, 113.
4. Blackley, D. C.; Charnock, R. S. J Int Rubber Ind 19737, 60.
5. Nielsen, L. E. Mechanical Properties of Polymers and Composites; Marcel Dekker: New York, 1974; Vol. 1.
6. Danesi, C. S.; Porter, R. S. Polymer 1978, 19, 448.
7. Dao, K. C. Polymer 1984, 25, 1527.
8. Baer, M. J Appl Polym Sci 1972, 16, 1109.
9. Varughese, H.; Bhagavan, S. S.; Someswara Rao, S.; Thomas, S. Eur Polym J 1995, 31, 957.
10. Koshy, A. T.; Kuriakose, B.; Thomas, S.; Varughese, S. Polymer 1993, 34.
11. George, S.; Neelakantan, N. R.; Varughese, K. T.; Thomas, S. J Appl Polym Sci, Part B: Polym Phys 1997, 35, 2309.
12. Porter, D. Group Interaction Modelling of Polymer Properties; Marcel Dekker: New York, 1995.
13. Ashby, M. F. Acta Metall 1989, 37, 1273.
14. Ferry, J. D. Viscoelastic Properties of Polymers, 3rd ed.; John Wiley: New York, 1980.
15. Mark, H. F.; Bikales, N.; Overberger, C. G.; Menges, G.; Kroschwitz, J. I. In Encyclopedia of Polymer Science and Engineering, 2nd ed.; John Wiley: New York, 1986; Vol. 5.
16. Thomas, S.; George A. Eur Polym J 1992, 28, 145.
17. Bernstein, R. E.; Paul, D. R.; Barlow, J. W. Polym Eng Sci 1976, 16, 593.
18. Murayama, T. Dynamic Mechanical Analysis of Polymeric Material; Elsevier: New York, 1978.
19. Varkey, J. T.; Augustine, S.; Groennickx, G.; Bhagavan, S. S.; Rao, S. S.; Thomas, S. J Polym Sci, Part B: Poly Phys 2000, 38, 2189.
20. Neumann, C.; Loveday, D. R.; Abetz, V.; Stadler, R. Macromolecules 1998, 31, 2493.
21. Sanchis, A.; Prolongo, M. G.; Masegosa, R. M.; Rubio, R. G. Macromolecules 1995, 28, 2693.
22. Watanabe, H. T. Chemtracts-Macromolecular Chemistry 1991, 2, 139.
23. Bhagawan, S. S.; Bandyopadhyay, G. G. J Natu Rubb Research 1996, 9, 100/
24. Varkey, J. T.; Rao, S. S.; Thomas, S. J Appl Polym Sci 1995, 56, 451.
25. Varkey, J. T.; Rao, S. S.; Thomas, S. Polym Plast Technol Eng 1996, 35, 1.

26. Varkey, J. T.; Rao, S. S.; Thomas, S. J Appl Polym Sci 1996, 62, 2169.
27. Varkey, J. T.; Chatterji, P. R.; Rao, S. S.; Thomas, S. J Appl Polym Sci 1998, 68, 1473.
28. Varkey, J. T.; Rao, S. S.; Thomas, S. Polymers Polym Compo 1998, 6, 237.
29. Varkey, J. T.; Rao, S. S.; Thomas, S. Plast Rubb Compos Process Appl 1995, 24, 249.
30. Blackley, D. C. Polymer Latices: Science and Technology, 2nd ed.; Kluwer Academic: New York, 1997; Vol. 2.
31. Walsh, D. J.; Higgins, J. S. Polymer 1982, 23, 336.
32. Blackley, D. C. Polymer Latices: Science and Technology, 2nd ed.; Kluwer Academic: New York, 1997; Vol. 3.
33. King, P. Lecture given to London Section of the United Kingdom Plastic and Rubber Institute, December 1980.
34. Popoola, K. A. Ph.D. Dissertation, UK Council for National Academic Awards.
35. Walsh, D. J.; Higgins, J. S. Polymer 1982, 23, 336.
36. Perera, M. C. S.; Ishiaku, U. S.; Ishak, Z. A. M. Eur Polym J 2001, 37, 167.
37. Perera, M. C. S.; Ishiaku, U. S.; Ishak, Z. A. M. Polym Degrad Stabili 2000, 68, 393.
38. Aklonis, J. J.; Macknight, W. J.; Shen, M. Introduction to Polymer Viscoelasticity; John Wiley: New York, 1972.
39. William, M. L.; Landel, R. F.; Ferry, J. D. J Am Chem Soc 1954, 77, 3701.
40. Alcoutlabi, M.; Martinez-Vega, J. J. Polymer 1998, 39, 6269.
41. Wismie, C.; Maria, G.; Monge, P. Eur Polym J 1985, 21, 479.
42. Whitney, J. M.; McCullough, R. L. In Delaware Composites Design Encyclopedia; Technomic Publishing: Lancaster, UK, 1990; Vol. 2.
43. Shick, R. A.; Ishida, H. In Characterisation of Composite Materials; Butterworth-Heinemann: Boston, 1994; Chap. 8, pp 147–183.
44. Mazich, K. A.; Killogoar, Jr., P. C.; Ingram, J. A. Rubber Chem & Tech 1989, 62, 305.
45. Mazich, K. A.; Plummer, Jr., H. K.; Samus, M. A.; Killogoar, Jr., P. C. J Appl Polym Sci 1989, 37, 1877.
46. Kerner, E. H. Proc Phys Soc, London, Sec B 1956, B69, 808.
47. Nielson, N. E. Rheol Acta 1974, 13, 86.
48. Halpin, J. C. J Compos Mater 1970, 3, 732.
49. George, S.; Joseph, R.; Varughese, K. T.; Thomas, S. Polymer 1995, 36, 4405.